

Structural basis of the lisinopril-binding specificity in N- and C-domains of human somatic ACE[☆]

Jorge H. Fernandez,^{a,b} Mirian A.F. Hayashi,^a Antonio C.M. Camargo,^a
and Goran Neshich^{b,*}

^a Center of Applied Toxinology, Instituto Butantan, SP, Brazil

^b Structural Bioinformatic Laboratory, CNPTIA-EMBRAPA, Campinas, SP, Brazil

Received 4 July 2003

Abstract

Angiotensin I-converting enzyme (ACE) is a dipeptidyl carboxypeptidase which converts angiotensin I into the vasopressor peptide angiotensin II and also inactivates the hypotensive peptide bradykinin, playing an important role in blood pressure regulation. The present work describes the molecular modeling of the N-terminal human somatic ACE in complex with the inhibitor lisinopril, identifying the residues involved in the inhibitor-binding pocket. The obtained results identify differences in the lisinopril lysine moiety-binding residues for N- and C-terminals of sACE domains and an important carboxy-terminal proline hydrophobic accommodations mediated by the aromatic ring of Tyr₅₃₂ and Tyr₁₁₂₈ residues, respectively. The present model will be useful for the development of a new inhibitor family based on the natural BPP peptides and derivatives, or even to improve the binding capacities and the domain specificity of the already known inhibitors.

© 2003 Elsevier Inc. All rights reserved.

Keywords: Angiotensin I-converting enzyme; Somatic ACE; BPPs; Lisinopril; Homology modeling

The angiotensin I-converting enzyme (ACE, EC 3.4.15.1) plays a key role in the cardiovascular homeostasis and regulation of blood pressure, by generating the potent vasoconstrictor angiotensin II (A-II) after cleavage of the C-terminal dipeptide from angiotensin I (A-I) [1,2]. In addition, the ACE inactivates the bradykinin, blocking its hypotensive effects [3,4]. The discovery of the natural inhibitors of ACE isolated from Brazilian snake venoms [5–7] allowed the development of several highly potent and specific ACE inhibitors widely employed as orally active drugs for the treatment of hypertension, cardiac failure, and diabetic nephropathies [8,9].

ACE is mainly expressed as a somatic isoform that is an ectoenzyme found on the surface of vascular endothelial, epithelial, and neuroepithelial cells [8], and as a

germinal form found in male developing spermatidis and in mature sperm, the testis-specific ACE (tACE) [10–13]. The somatic ACE (sACE) displays two highly homologous active sites, one at the C-domain (sACEc) and another at the N-domain (sACEn) of the protein, each of which is catalytically active and functionally independent [14]. Although the two domains are highly efficient to convert A-I into A-II and to inactivate Bk [15], the N-site is several times more efficient in hydrolyzing the peptides angiotensin 1–7 [16] and the AcS-DKP, a negative regulatory factor of the hematopoietic stem cell differentiation and proliferation [17]. More recently, we have shown that some natural inhibitors of ACE were also able to selectively block the N- and C-terminal active sites of the sACE [18,19]. Both the human sACE and tACE are encoded by the same gene [4]. Indeed, the tACE corresponds to the C-domain of the sACE with an additional N-terminal sequence [12]. In human tACE, amino acid residues 68–732 are identical to the residues 642–1306 of the human sACE. In spite of a very similar active site sequence (including a highly conserved motif HEXXH), distinct peptide hormone

[☆] *Abbreviations:* ACE, angiotensin I-converting enzyme; sACE, somatic ACE; tACE, testicular or germinal ACE; A-I, angiotensin I; A-II, angiotensin II; Bk, bradykinin; BPPs, Bk-potentiating peptides; Cl⁻, chloride ion.

* Corresponding author. Fax: +55-19-3789-5743.

E-mail address: neshich@cbi.cnptia.embrapa.br (G. Neshich).

substrates have been found for each active site of the sACE and tACE. Other common substrates are cleaved at different rates [15,17].

Each sACE active site seems to be relevant for distinct physiological function [14–17], and the development of selective inhibitors has been employed in order to specifically probe each function [20]. However, the recent description of the crystal structure of the *Drosophila* AnCE [21] and human tACE [22] provided a new possibility to access this question. In this work, we describe the molecular model of the N-domain active site of human sACE (sACEn) and the analysis of lisinopril and sACEn complex obtained by homology modeling. We used Modeller [23] for simultaneous modeling of the sACEn–lisinopril complex with zinc (Zn), chloride cofactors (Cl^-), and important structural waters in the active site. The Java Protein Dossier (SMS 3.0) [24] was used for the initial analysis of hydrogen bonds including structurally important water molecules and electrostatic interactions. The refinement of the obtained model using energy minimization and restrained molecular dynamics in Gromacs 3.0 [25] was the second step of our work, and the obtained sACEn–lisinopril interactions were compared to the already described ones in the initial model. The data presented here may aid enzymological studies by rationalizing the design of specific inhibitors for each active site, as well as provide an important tool to study the physiological function of each domain in the regulation of blood pressure and other events involving activity of ACE isoforms.

Materials and methods

Alignments. Sequences of the N- and C-domains of the human somatic angiotensin I-converting enzyme (sACE, P12821 [26]) and human testicular ACE (tACE [22]) were aligned using ClustalW [27] software. The alignment was further refined by removing the first 42 N-terminal and the last 76 C-terminal amino acids of the sACE sequence and used in the modeling procedure.

Modeling. The structure of the human tACE complexed with lisinopril (pdb 1o86) [22] has been used to predict the three-dimensional (3D) structure of the C- and N-terminal domains of human sACE. We have taken advantage of the 100% sequence identity between tACE and sACEc to directly map the sACEc sequence in the 3D structure described for tACE in the 1o86 structure. The atomic coordinates of the 1o86 pdb structure, solved at 2.0 Å resolution, were used as a template in comparative modeling by satisfaction of spatial restraints [23] implemented in the program Modeller 6v2 [28]. The program uses methods of conjugated gradients and CHARMM [29] energy terms for molecular dynamics with simulated annealing [30]. In the sACEn modeling procedure, we generated 25 different models of the protein structure. The quality of the predicted fold was evaluated in Modeller using the score of the variable target function method [28]. The stereochemical quality of the five best scoring models was assessed by Procheck program [31] at the same resolution as the 1o86 structure. The final model was selected based on the overall stereochemical quality. Using the same modeling procedure, the sACEn structure was modeled in complex with Zn, Cl^- ions, structural waters, and lisinopril inhibitor. The obtained model was subjected to energy minimization using Gromacs [25].

Energy minimization of the complex using Gromacs. To refine the molecular model of the sACEn–lisinopril complex, additional energy minimization and equilibrating molecular dynamics simulations were carried out with the program Gromacs 3.0 [25] on a dual-CPU Intel PIII Linux workstation. Initial sACEn protein model was submitted to a steepest-descent (SD) energy minimization (1000 steps) to remove bad van der Waals contacts. In parallel, the Gromacs topology of the lisinopril ligand was obtained in the PRODRG server [32]. To direct the docking of the lisinopril to the minimized sACEn, the already modeled structure of the complex was used (Fig. 3A). The obtained structure of the complex was used in a second SD energy minimization (3000 steps) and for further relaxation, a restrained molecular dynamic was performed for 50 ps with Berendsen-type temperature (300 K) and pressure (1 atm) coupling in a $40 \times 40 \times 40$ simulation cell [25,33,34], implementing the PME method [35]. An unrestrained multiple step conjugate-gradient (CG) minimization process was used ($0.1 \text{ kJ mol}^{-1} \text{ nm}^{-1}$) to obtain the minimized structure of the complex.

Evaluation of interactions in sACE–lisinopril complex. In modeling procedures we have created conditions for the comparison of binding pocket with those of sACEn and sACEc–lisinopril. For evaluation of the sACE–lisinopril and sACE– Cl^- interactions, the Java Protein Dossier (JPD) program of the Sting Millennium Suite (SMS 3.0) [24] was used. The cutoff distances for hydrogen bonds, salt bridges, and aromatic interactions were 2–3.2, 2–6, and 4.0 Å, respectively. For the superimposition of N- and C-terminal sACE modeled domain backbones, combinatorial extension method (CE) [36] and PsISM program [37] were used.

Results and discussion

Sequence alignment

The aligned sequences of N- and C-terminal domains of sACE are represented in Fig. 1. There were 2 gaps with a total of 5 insertions included and 265 differences between the two domains over the 592 aligned residues, representing 55% of sequence identity. The secondary structure elements described for tACE [22] identical to sACEc were mapped in the alignment. A lower conservation of amino acids was mainly found at the α -helix₁ (α_1) to 3–10-helix₃ (H_3) and at α_{18} to α_{20} secondary structure elements (Fig. 1). The central sequence of the domains (at α_8 to H_7 elements), containing and surrounding the active site (HEXXH motif), is more conserved. The observed overall identity and relative residue conservation in the secondary structure elements predicted for sACEn, if compared to that of the tACE structure (sACEc in our alignment), makes the comparative modeling of sACEn domain feasible.

Overall description of the sACEn initial model

The SMS Ramachandran plot [24] for the modeled complex sACEn–lisinopril (Fig. 2) shows 93.9% of the residues in the most favorable regions, 5.0% in additional allowed regions, and 1.2% in generously allowed regions. No residues lie in the disallowed regions and stereochemical parameters checked in Procheck [31] were inside or better than expected at 95% confidence level.

ACE Sequence: gi|113045|sp|P12821|ACE_HUMAN Angiotensin I-converting enzyme, somatic isoform precursor

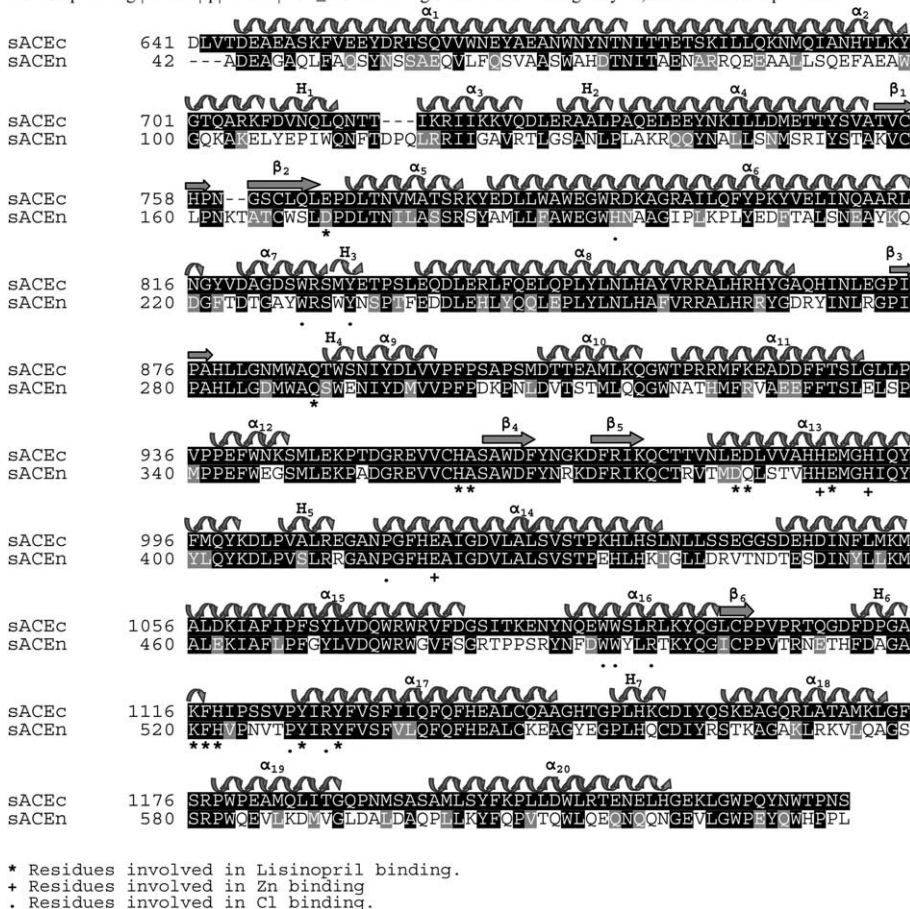


Fig. 1. Sequence alignment of C (sACEc) and N-domains (sACEn) of human sACE, Clustal W [28] alignment was used as input in the modeling procedure. Identical residues (55%) are represented in a black background. Secondary structure elements are represented on the top of the alignment (α , α -helices, β , β -strands, H, and 3–10-helices) according to the resolved tACE crystal structure [23]. On the bottom of the alignment are marked the important residues that are involved in the lisinopril (*), Zn (+), and Cl⁻ (.) binding.

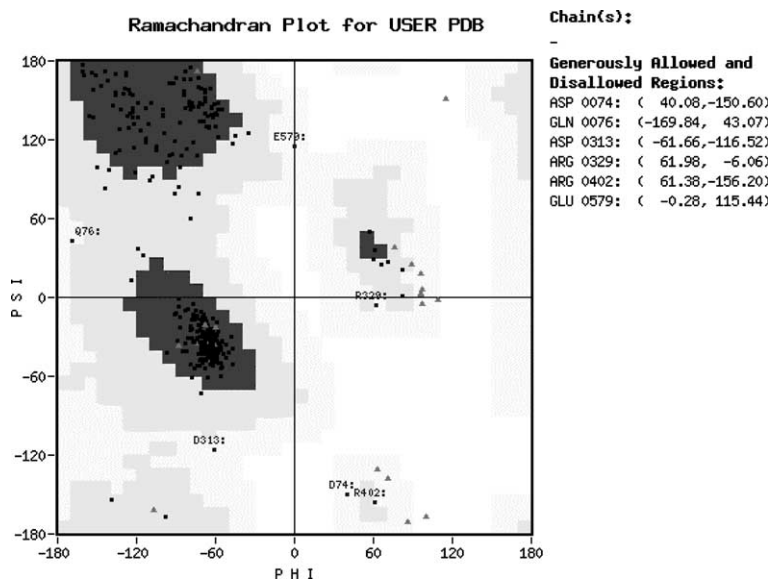


Fig. 2. SMS Ramachandran plot [25] for the sACEn model. The residues displayed on the right are located in the generously allowed regions. No residue is located in the disallowed regions. Glycine residues are displayed as triangles.

Predicted sACEn fold maintains the overall structure of ellipsoid shape with a central groove already described for human tACE [23] and *Drosophila* AnCE [21]. The secondary structure of modeled sACEn was calculated using the DSSP program [38] and it is composed of 21 α -helices, six 3–10-helices, and six antiparallel β -strands. The most important differences between the tACE and *Drosophila* AnCE secondary structures (in Fig. 1) were the lack of the 3–10-helix structure at the H₁ position, the lateral addition of the Met₃₄₉ to the β -barrel formed by β_4 - and β_5 -strands, and the insertion of a small α -helix at His₅₂₂–Asn₅₂₅ positions. The backbone

superimposition of sACEn initial model and tACE structures using CE program [36] and PrISM [37] showed backbone rmsd equal to 0.3 and 0.4 Å, respectively, indicating high conservation in the initial model domain structure. The zinc ion, critical for the catalysis, is coordinated by the conserved His₃₉₂, His₃₉₆, Glu₄₂₀, and carboxylic group of the lisinopril inhibitor (Fig. 3A) in a penta-coordinated geometry. The additional Glu₃₉₃ from the HEXXH zinc-binding motif, conserved in the sequence of the gluzincin family of metalloproteases, interacts directly with the carboxylic moiety of lisinopril and coordinates the position of the important catalytic

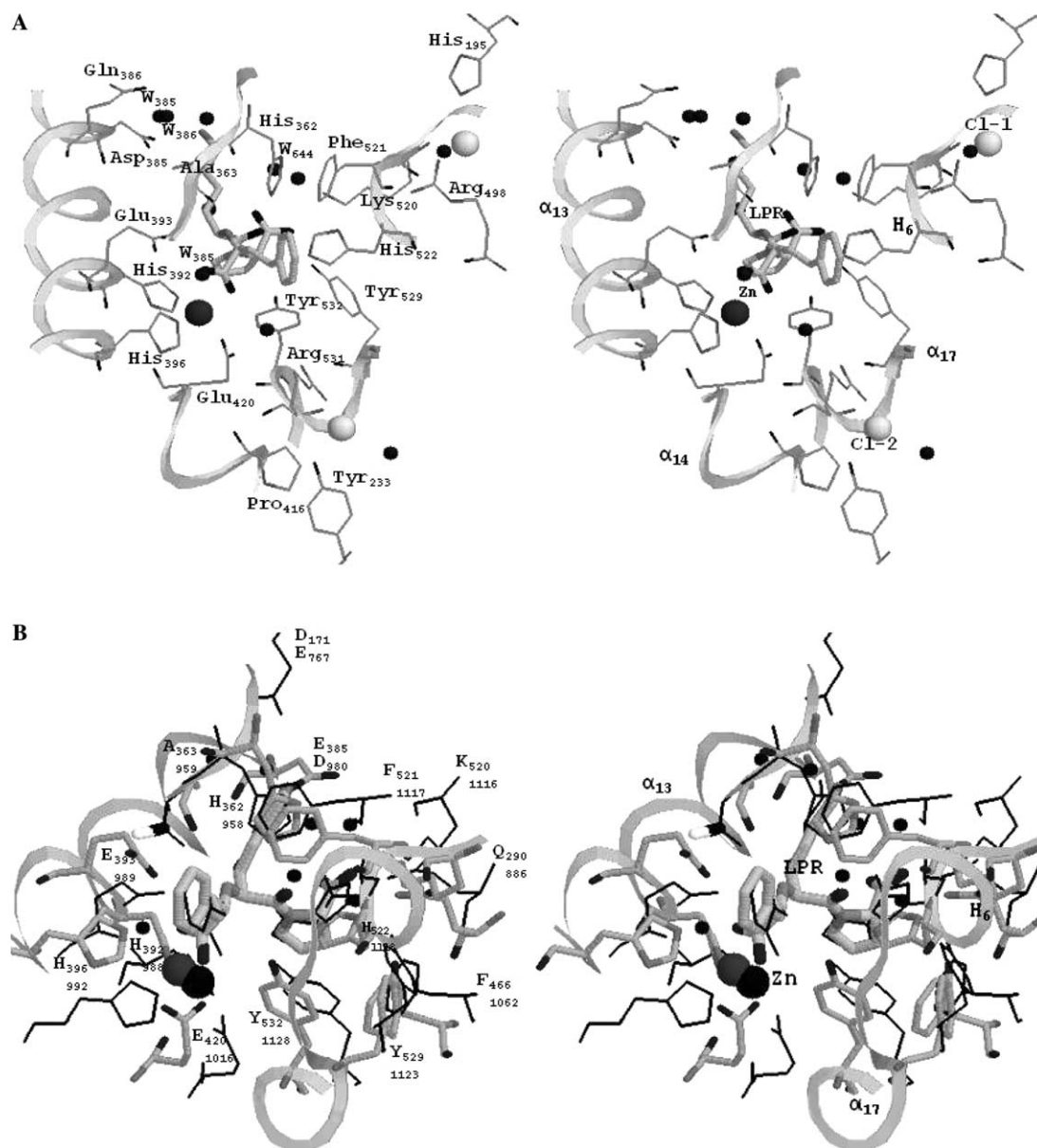


Fig. 3. Structural model of the active site of human sACEn and residues responsible for lisinopril binding. (A) Stereo representation of the sACEn active site and important residues contacting lisinopril inhibitor (LPR), Zn cofactor (Zn), and Cl⁻ ions (Cl-1 and Cl-2). Important structural waters (w) are represented as small dark spheres. (B) Superimposed structures of the binding pockets of human sACEn–lisinopril minimized complex (thick line, upper labeled residues) and C-domain (thin dark line, lower labeled residues).

water molecule (W₃₈₅) placed near the enzyme active center (Fig. 3A). A similar zinc cofactor–inhibitor interaction in penta-coordinated geometry was described in tACE–lisinopril complex (pdb 1o86) [22] and AnACE–lisinopril complex [21].

Lisinopril–sACE_N interactions in the initial model

Lisinopril is a carboxylic inhibitor of ACE that binds to human sACE with $K_i = 0.39$ nM [39] and appears to mimic peptide substrates. The main interactions between sACE_N and lisinopril inhibitor are ionic and hydrogen bonds and aromatic stacking (Table 1 and Fig. 3A). The active sites of the enzyme are placed in the α_{13} -helix (HEXXH motif) and α_{14} -helix (Glu₄₂₀ residue in Fig. 3A) that coordinated zinc ion and catalytic water molecule. However, the lisinopril-binding pocket is completed by the α_{17} - and H₆-helices and the 360–363 loop residues (Fig. 3A). The Java Protein Dossier program [24] was used to identify the lisinopril-binding pocket. The obtained interactions and distances are shown in Table 1.

The accommodation of the lisinopril carboxy-terminal proline moiety is mediated by the hydrophobic interaction with the aromatic ring of the Tyr₅₃₂ and by the lateral hydrophobic pocket formed by aromatic rings of Tyr₅₂₉, Phe₄₆₆, and Phe₅₂₁. The lisinopril lysine moiety is contacted by the Gln₃₈₆ and Asp₃₈₅ residues through the water mediated hydrogen bonds besides charge attractive contact with Asp₃₈₅. The lisinopril amino-terminal phenyl moiety is accommodated by the aromatic

stacking with the Phe₅₂₁ residue. The His₃₆₁ and Ala₃₆₂, contacting the amino and carboxyl groups of the S2'–S1' peptide bond, and the Glu₃₉₃ contacting the carboxylic lisinopril moiety, are positioned in a ring form, comprising the α_{13} , α_{17} , H₆, and the 360–365 loop positions (Fig. 3A).

The residues coordinating lisinopril lysine moiety in our sACE_N model are different from those described in the tACE–lisinopril complex [22] (see sACE_C in Table 1), although the position of the inhibitor is mainly unchanged in the superposition of the sACE_N and sACE_C–lisinopril complexes (Fig. 3B).

Chloride-binding site of human sACE_N

The location of the chloride ions in the modeled human sACE_N and the enzyme interacting residues was determined using the Ligand Pocket function in the Java Protein Dossier (SMS 3.0) [24] and the obtained results are given in Table 2.

Recently, it has been proposed that the chloride ions might interact with the substrate [40]. Although Cl[−] dependence of hydrolysis is substrate specific, the chloride ion location at 20 Å for Cl-1 and 10 Å for Cl-2 (see Fig. 3A for Cl[−] nomenclature) from the active site makes a direct interaction with short peptides unlikely [22]. Moreover, Cl-2 is located in the N-cavity and may directly help in the accommodation of the substrate in the active site. Similarly as described for the tACE [22], and also mapped in the sACE_C, the primary ligand for Cl-2 in modeled sACE_N is Arg₅₃₁, located in the

Table 1

Contacts between lisinopril and sACE-N- and C-domain residues and mapped distances in the Java Protein Dossier program [25]

Position	Lisinopril	sACE-C	Distance (Å)	sACE-N	Distance (Å)	sACE-N minimized	Distance (Å)
S1	Aromatic ring	Ring-Phe ₁₁₁₇	3.7	Ring-Phe ₅₂₁	3.8	Ring-Phe ₅₂₁	3.6
0	COOH-(C=O)	W ₇₄₇	2.8 ^a	W ₆₃₂	2.8	—	—
0	COOH-(C=O)	OE2-Glu ₉₈₉	2.7 ^a	OE2-Glu ₃₉₃	2.7	OE2-Glu ₃₉₃	3.6
0	COOH-(C=O)	W ₇₄₇ –OE2-Glu ₉₈₉	2.8–3.2	W ₃₈₅ –OE2-Glu ₃₉₃	2.8–3.2	—	—
0	COOH(O [−])	OH-Tyr ₁₁₂₈	2.8 ^a	OH-Tyr ₅₃₂	2.7	OH-Tyr ₅₃₂	2.9
0	COOH(O [−])	Zn	2.1 ^a	Zn	2.3	Zn	2.0
S1'	Lys-(NH ₂)	W ₃₈₅ –OD1-Asp ₉₈₂	3.3–2.9 ^a	W ₆₇₁ –OD1-Gln ₃₈₆	3.0–2.9	OD1-Gln ₃₈₆	4.6
S1'	Lys-(NH ₂)	W ₇₈₇ –OD1-Asp ₉₈₂	3.0–2.7 ^a	W ₇₁₈ –OD1-Asp ₃₈₅	3.2–2.7	OD1-Asp ₃₈₅	3.7
S1'	Lys-(NH ₂)	OE2-Glu ₇₆₇	3.4 ^a	OE2-Asp ₁₇₁	5.0	OE2-Asp ₁₇₁	4.3
S1'	Lys-(NH ₂)	W ₁₀₃₈	3.5 ^a	W ₉₁₅	3.1	—	—
S1'	C α -(NH)	O-Ala ₉₅₉	2.9 ^a	O-Ala ₃₆₃	2.9	O-Ala ₃₆₃	2.3
S1'	C α -(NH)	OE-Glu ₉₈₉	3.4	OE-Glu ₃₉₃	3.4	OE-Glu ₃₉₃	2.3
S1'	C α -(C=O)	NE2-His ₉₅₈	2.8 ^a	NE2-His ₃₆₂	2.7	NE2-His ₃₆₂	2.1
S1'	C α -(C=O)	NE2-His ₁₁₁₈	3.1 ^a	NE2-His ₅₂₂	3.1	NE2-His ₅₂₂	2.5
S2'	Pro-(C=O)	W ₈₆₆	2.8 ^a	W ₇₄₉	2.8	—	—
S2'	Pro-(C=O)	W ₇₅₉ –NZ-Lys ₁₁₁₆	2.7–3.0 ^a	W ₆₄₄ –NZ-Lys ₅₂₀	2.7–3.0	NZ-Lys ₅₂₀	3.1
S2'	Pro-(O [−])	NZ-Lys ₁₁₁₆	2.9 ^a	NZ-Lys ₅₂₀	2.9	NZ-Lys ₅₂₀	2.0
S2'	Pro-(O [−])	OH-Tyr ₁₁₂₅	2.6 ^a	OH-Tyr ₅₂₉	2.7	OH-Tyr ₅₂₉	3.2
S2'	Pro-ring	Ring-Tyr ₁₁₂₅	3.6	Ring-Tyr ₅₂₉	3.6	Ring-Tyr ₅₂₉	3.7

In the comparison are included mapped distances in the initial model, including structural waters (sACE-N) and final model (sACE-N minimized). Principal differences between N- and C-domains are shaded in gray.

^a According to [23].

Table 2

Contacts between sACE-N- and C-domain residues and Cl⁻ ions mapped in Java Protein Dossier program [25]

	sACE-C	Distance (Å)	sACE-N	Distance (Å)
Cl-1	W ₇₅₅ -(C=O)Cα-Asp ₁₁₁₁	3.2–2.8	W ₆₄₀ -(C=O)Cα-Asp ₅₁₆	3.2–2.8
Cl-1	NE-Arg ₇₉₁	3.2	NE-His ₁₉₅	3.1
Cl-1	NH-Arg ₇₉₁	3.4	—	—
Cl-1	NH-Arg ₁₀₉₄	3.2	NE-Arg ₄₉₈	3.2
Cl-1	NE-Trp ₁₀₉₀	3.3	NE-Trp ₄₉₄	3.3
Cl-1	Ring-Trp ₁₀₉₁	3.6	Ring-Trp ₄₉₅	3.6
Cl-2	W ₅₉₁ -(C=O)Cα-Trp ₈₂₅	3.1–2.9	W ₅₉₁ -(C=O)Cα-Trp ₂₂₉	3.1–2.9
Cl-2	OH-Tyr ₈₂₉	3.0	OH-Tyr ₂₃₃	3.0
Cl-2	NE-Arg ₁₁₂₇	3.0	NE-Arg ₅₃₁	3.0
Cl-2	NH-Arg ₁₁₂₇	3.5	NH-Arg ₅₃₁	3.5
Cl-2	(NH)Cα-Arg ₁₁₂₇	3.6	(NH)Cα-Arg ₅₃₁	3.6
Cl-2	Ring-Pro ₁₀₁₂	3.6	Ring-Pro ₄₁₆	3.6
Cl-2	Ring-Pro ₁₁₂₄	3.6	Ring-Pro ₅₂₈	3.6

Principal differences are shaded in gray.

α₁₇-helix, in the vicinity of the residues Tyr₅₃₂ and Tyr₅₂₉, which also directly interact with lisinopril (Fig. 3A).

Model refinement and complex interaction analysis

To avoid the natural consequence of the homology modeling procedure (the possible targeting of the initial 3D structure to the obtained model) we performed an additional energy minimization and restrained MD in the initial model of the sACE_N-lisinopril complex in GROMACS [25]. The obtained minimized complex maintains the overall enzyme structure (sACE_N rmsd = 1.5 Å), all the described sACE-lisinopril contacts, and the overall position of the LPR inhibitor (LPR rmsd = 0.3 Å). The obtained structure of the ligand pocket residues is showed in Fig. 3B. The Java Protein Dossier program [24] was used to identify the lisinopril-binding pocket in minimized complex. In the MD process we lost the information about the forming H-bond water molecules, and for that, all water molecules were removed for interaction analysis in the final model. The obtained interactions and distances are shown in Table 2.

In newly analyzed contacts of the minimized ligand pocket residues, the only differences with the already mapped were the stabilization of the salt bridges between lisinopril lysine moiety and Glu₃₈₅, and carboxylic group of the lisinopril proline moiety and Gln₂₉₀. The Phe₄₆₆ position in the enzyme hydrophobic pocket (Fig. 3B) is also noticeable. All these contacts (Table 2) are maintained in 500 ps restrained and 100 ps unrestrained MD processes (not described in this paper).

Substrate specificity of sACE-N- and C-domains

The N- and C-domains of sACE are a good model system for investigating the basis of the substrate specificity in the gluzincin family of metalloproteases. Distinct binding affinities for each domain were previously

reported for natural substrates such as A-I and Bk, and also for inhibitors such as BPPs [14,18,19].

The sACE active sites are located in the center of the large internal channel, as already described for AnCE [21] and tACE [22]. The described ligand-binding residues and catalytic Zn ion divided the channel in two different clefts. The carboxy-terminal side of the substrate-inhibitor is accommodated in the small C-chamber and the amino-terminal side in the large N-chamber. Analysis of the substrate-binding channel indicated that the lengths of the N- and C-site chambers are approximately 17 and 8 Å, respectively (data not shown). It is possible that the channel length is the limiting factor for the binding and hydrolysis of longer peptides. The length restriction might be primarily on the substrate sequence N-terminal to the cleavage site, due to the natural dicarboxydipeptidase activity of the sACE.

As shown in Fig. 3A, the Tyr₅₃₂ presents a hydrophobic stacking with the lisinopril S2' proline while the Pro ring is nearly perpendicular to the Tyr₅₃₂ aromatic ring at 3.6 Å. This stacking is strongly maintained in the sACE_C-lisinopril model (Fig. 3B and Table 1) and in tACE-lisinopril structure [22], and reminds of an off-centered parallel orientation of side chain aromatic groups in π-stacking interactions [41]. Proline-aromatic rings hydrophobic stacking were described in the bradykinin-polyphenol complexes studied by NMR [42] and are the predominant mode of complexation of tannins by the salivary proline-rich proteins (PRPs) which are secreted into the oral cavity [43].

The hydrophobic patch provided by the aromatic rings of Tyr₅₃₂ in sACE_N and Tyr₁₁₂₈ in sACE_C (Tyr_{532,1128}), Phe_{521,1117}, Phe_{466,1062}, and Tyr_{527,1123} interacting with the S2' inhibitor position may explain why sACE generally favors a hydrophobic residue at the carboxy-terminal position of the substrate-inhibitors [14,19]. At the same time, tyrosine residues could interact with different types of substrate side-chain groups due to the aromatic-hydrophilic duality of their side

chain groups, indicating inherent interaction flexibility in α_{17} -helix (Fig. 3A).

Some of the sACE-C-domain residues altered in sACE-N-domain-binding pocket appear well positioned to interact with the lysine moiety of lisinopril inhibitor. The residue Gln₃₈₆–Asp₉₈₁ variation could create an electrostatically less favorable binding surface for the negatively charged residues at the inhibitor S1 contacting position, but would not change the accommodation of the lysine hydrogen bond through the structural important waters and the formed salt bridge with Glu₃₈₅ (sACE_N) or Glu₇₆₇ (sACE_C) (Figs. 3A and B). The lisinopril access to the active site across the channel may be different for C- and N-terminal domains. Although lisinopril-binding pocket is very similar in both sACE_N and sACE_C models, the already described K_i differences for each active site [14] may be explained by the electrostatic or hydrophobic properties that distinct residues are mapping to the channel surface. In addition, the N- and C-domain positions in sACE model suggest that the interdomain interactions may also play an important role in the substrate access to the active site (data not shown).

Our study and comparison of the overall topology of the human tACE and *Drosophila* AnCE crystal structure, and models for human sACE-N- and C-domains, bring new insights into the ACE active sites. This in turn can be used for the rational structure-based development of highly selective new drugs. These results will help to design more specific sACE inhibitors each targeting one of the sACE active sites.

Acknowledgments

This work was funded by Center of Applied Toxinology (CAT-CEPID), supported by a grant of the Fundação de Amparo à Pesquisa de São Paulo (FAPESP). We thank Dr. Bernard Maigret of the Université de Nancy for valuable discussion in MD experiments and Christian Baduert for helping in J.P.D. manipulation and data collection.

References

- [1] L.T. Skeggs, J.R. Kahn, N.P. Shumway, The preparation and function of hypertensin-converting enzyme, *J. Exp. Med.* 103 (1956) 295–299.
- [2] C.R. Esther Jr., E.M. Marino, T.E. Howard, P. Corvol, M.R. Capecchi, K.E. Bernstein, The critical role of the tissue angiotensin-converting enzyme as revealed by gene targeting in mice, *J. Clin. Invest.* 99 (1997) 2375–2385.
- [3] W. Linz, G. Wiemer, P. Gohlke, T. Unger, B.A. Scholkens, Contribution of kinins to the cardiovascular actions of angiotensin-converting enzyme inhibitors, *Pharmacol. Rev.* 47 (1) (1995) 25–49.
- [4] E. Villar, F. Soubrier, Molecular biology and genetics of the angiotensin-I-converting enzyme: potential implications in cardiovascular diseases, *Cardiovasc. Res.* 32 (1996) 999–1007.
- [5] S.H. Ferreira, M. Rocha e Silva, Potentiation of bradykinin and eledoisin by BPF (bradykinin potentiating factor) from *Bothrops jararaca* venom, *Experientia* 21 (1965) 347–349.
- [6] S.H. Ferreira, L.H. Greene, V.A. Alabaster, Y.S. Bakhle, J.R. Vane, Activity of various fractions of bradykinin potentiating factor against angiotensin I converting enzyme, *Nature* 225 (230) (1970) 79–80.
- [7] S.H. Ferreira, D.C. Bartelt, L.J. Greene, Isolation of bradykinin-potentiating peptides from *Bothrops jararaca* venom, *Biochemistry* 9 (13) (1970) 2583–2593.
- [8] M.A. Ondetti, D.W. Cushman, Inhibitors of angiotensin-converting enzyme, in: R.L. Soffer (Ed.), *Biochemical Regulation of Blood Pressure*, Wiley, New York, 1981, pp. 165–204.
- [9] B. Waebel, J. Nussberger, H.S. Brunner, in: Laragh, Brenner (Eds.), *Hypertension: Pathophysiology, Diagnosis and Management*, Raven Press, New York, 1990.
- [10] H.A. El-Dorry, H.G. Bull, K. Iwata, N.A. Thornberry, E.M. Cordes, R.L. Soffer, Molecular and catalytic properties of rabbit testicular dipeptidyl carboxypeptidase, *J. Biol. Chem.* 257 (1982) 14128–14133.
- [11] A.L. Lattion, F. Soubrier, J. Allegrini, C. Hubert, P. Corvol, F. Alhenc-Gelas, The testicular transcript of the angiotensin I-converting enzyme encodes for the ancestral, non-duplicated form of the enzyme, *FEBS Lett.* 252 (1989) 99–104.
- [12] M.R.W. Ehlers, E.A. Fox, D.J. Strydom, J.F. Riordam, Molecular cloning of human testicular angiotensin-converting enzyme: the testis isozyme is identical to the C-terminal half of endothelial angiotensin-converting enzyme, *Proc. Natl. Acad. Sci. USA* 86 (1989) 7741–7745.
- [13] R.S. Kumar, J. Kusari, S.N. Roy, R.L. Soffer, G.C. Sen, Structure of testicular angiotensin-converting enzyme: a segmental mosaic enzyme, *J. Biol. Chem.* 264 (1989) 16754–16758.
- [14] L. Wei, E. Clauser, F. Alhenc-Gelas, P. Corvol, The two homologous domains of human angiotensin I-converting enzyme interact differently with competitive inhibitors, *J. Biol. Chem.* 267 (19) (1992) 13398–13405.
- [15] E. Jaspard, L. Wei, F. Alhenc-Gelas, Differences in the properties and enzymatic specificities of the two active sites of angiotensin I-converting enzyme (kininase II). Studies with bradykinin and other natural peptides, *J. Biol. Chem.* 268 (1993) 9496–9503.
- [16] P.A. Deddish, B. Marcic, H.L. Jackman, H.Z. Wang, R.A. Skidgel, E.G. Erdos, N-domain-specific substrate and C-domain inhibitors of angiotensin-converting enzyme: angiotensin-(1-7) and keto-ACE, *Hypertension* 31 (1998) 912–917.
- [17] A. Rousseau, A. Michaud, M.T. Chauvet, M. Lenfant, P. Corvol, The haemoregulatory peptide *N*-acetyl-Ser-Asp-Lys-Pro is a natural and specific substrate of the N-terminal active site of human angiotensin-converting enzyme, *J. Biol. Chem.* 270 (1995) 3656–3661.
- [18] J. Cotton, M.A. Hayashi, P. Cuniasso, G. Vazeux, D. Ianzer, A.C. Camargo, V. Dive, Selective inhibition of the C-domain of angiotensin I converting enzyme by bradykinin potentiating peptides, *Biochemistry* 41 (19) (2002) 6065–6071.
- [19] M.A.F. Hayashi, A.F. Murbach, D. Ianzer, F.C.V. Portaro, B.C. Prezoto, P.F. Silveira, C.A. Silva, R.S. Pires, L.R.G. Britto, V. Dive, A.C.M. Camargo, The C-type natriuretic peptide precursor of snake brain contains highly specific inhibitors of the angiotensin-converting enzyme, *J. Neurochem.* (2003) in press.
- [20] D. Georgiadis, F. Beau, B. Czarny, J. Cotton, A. Yiotakis, V. Dive, Roles of the two active sites of somatic ACE in the cleavage of angiotensin I and bradykinin. Insights from selective inhibitors, *Circ. Res.* (2003) submitted.
- [21] H.M. Kim, D.R. Shin, O.J. Yoo, H. Lee, J.O. Lee, Crystal structure of *Drosophila* angiotensin I-converting enzyme bound to captopril and lisinopril(1), *FEBS Lett.* 538 (2003) 65–70.

- [22] R. Natesh, S. Schwager, E. Sturrock, K. Acharya, Crystal structure of the human angiotensin-converting enzyme-lisinopril complex, *Nature* 421 (2003) 551–554.
- [23] A. Sali, T.L. Blundell, Comparative protein modelling by satisfaction of spatial restraints, *J. Mol. Biol.* 234 (1993) 779–815.
- [24] G. Neshich, R. Togawa, A. Mancini, P. Kuser, M. Yamagishi, G. Pappas, T. Campos, F. Luna, A. Oliveira, R. Miura, M. Inoue, L. Horita, F. Dominiquini, A. Álvaro, G. Gomes, E. Freitas, A. Mattiuz, S. Souza, C. Baudet, R. Higa, STING Millennium: a Web based suite of programs for comprehensive and simultaneous analysis of protein structure and sequence, *N.A.R.* 31 (13) (2003) 3386–3392.
- [25] E. Lindahl, B. Hess, D. van der Spoel, GROMACS 3.0: a package for molecular simulation and trajectory analysis, *J. Mol. Modeling* 7 (2001) 306–317.
- [26] F. Soubrier, F. Alhenc-Gelas, C. Hubert, J. Allegrini, M. John, G. Tregear, P. Corvol, Two putative active centers in human angiotensin I-converting enzyme revealed by molecular cloning, *Proc. Natl. Acad. Sci. USA* 85 (1988) 9386–9390.
- [27] J.D. Thompson, D.G. Higgins, T.J. Gibson, CLUSTAL W: improving the sensitivity of progressive multiple sequence alignment through sequence weighting, positions-specific gap penalties and weight matrix choice, *Nucleic Acids Res.* 22 (1994) 4673–4680.
- [28] A. Fiser, R.K. Do, A. Sali, Modeling of loops in protein structures, *Protein Sci.* 9 (2000) 1753–1773.
- [29] B.R. Brooks, R.E. Bruccoleri, B.D. Olafson, D.J. States, S. Swaminathan, M. Karplus, CHARMM: a program for macromolecular energy, minimization, and dynamics calculations, *J. Comp. Chem.* 4 (1983) 187–217.
- [30] M.A. Marti-Renom, A. Stuart, A. Fiser, R. Sánchez, F. Melo, A. Sali, Comparative protein structure modeling of genes and genomes, *Annu. Rev. Biophys. Biomol. Struct.* 29 (2000) 291–325.
- [31] R.A. Laskowski, M.W. MacArthur, D.S. Moss, J.M. Thornton, PROCHECK: a program to check the stereochemical quality of protein structures, *J. Appl. Cryst.* 26 (1993) 283–291.
- [32] D.M.F. van Aalten, R. Bywater, J.B.C. Findlay, M. Hendlich, R.W.W. Hooft, G. Vriend, PRODRG, a program for generating molecular topologies and unique molecular descriptors from coordinates of small molecules, *J. Comput. Aided Mol. Design* 10 (1996) 255–262.
- [33] M. Pellegrini, A.A. Bremer, A.L. Ulfers, N.D. Boyd, D.F. Mierke, Molecular characterization of the substance P*neurokinin-1 receptor complex: development of an experimentally based model, *J. Biol. Chem.* 276 (25) (2001) 22862–22867.
- [34] T.M. Louie, H. Yang, P. Karnchanaphanurach, X.S. Xie, L. Xun, FAD is a preferred substrate and an inhibitor of *Escherichia coli* general NAD(P)H:flavin oxidoreductase, *J. Biol. Chem.* 277 (42) (2002) 39450–39455.
- [35] U. Essman, L. Perela, M.L. Berkowitz, T. Darden, H. Lee, L.G. Pedersen, A smooth particle mesh Ewald method, *J. Chem. Phys.* 103 (1995) 8577–8592.
- [36] I.N. Shindyalov, P.E. Bourne, Protein structure alignment by incremental combinatorial extension (CE) of the optimal path, *Protein Eng.* 11 (9) (1998) 739–747.
- [37] A.S. Yang, B. Honig, Sequence to structure alignment in comparative modeling using PrISM, *Proteins: Struct., Funct. Genet.* 3 (1999) 66–72.
- [38] W. Kabsch, C. Sander, Dictionary of protein secondary structure: pattern recognition of hydrogen-bonded and geometrical features, *Biopolymers* 22 (1983) 2577–2637.
- [39] L. Wei, F. Alhenc-Gelas, P. Corvol, E. Clauser, The two homologous domains of human angiotensin I-converting enzyme are both catalytically active, *J. Biol. Chem.* 266 (1991) 9002–9008.
- [40] X. Liu, M. Fernandez, M.A. Wouters, S. Heyberger, A. Husain, Arg(1098) is critical for the chloride dependence of human angiotensin I-converting enzyme C-domain catalytic activity, *J. Biol. Chem.* 276 (36) (2001) 33518–33525.
- [41] G.B. McGaughey, M. Gagné, A. Rappé, π -Stacking interactions: alive and well in proteins, *J. Biol. Chem.* 273 (1998) 15458–15463.
- [42] N.J. Baxter, T.H. Lilley, E. Haslam, M.P. Williamson, Multiple interactions between polyphenols and a salivary proline-rich protein repeat result in complexation and precipitation, *Biochemistry* 36 (18) (1997) 5566–5577.
- [43] S. Verge, T. Richard, S. Moreau, A. Nurich, J.M. Merillon, J. Vercauteren, J.P. Monti, First observation of solution structures of bradykinin-penta-*O*-galloyl- β -glucopyranose complexes as determined by NMR and simulated annealing, *Biochim. Biophys. Acta* 1571 (2) (2002) 89–101.